

Clinical Investigation

Validity and Diagnostic Performance of Computing Fractional Flow Reserve From 2-Dimensional Coronary Angiography Images

Vahid Mohammadi, MD^{1,2}; Massoud Ghasemi, MD¹; Reza Rahmani, MD¹; Maryam Mehrpooya, MD¹; Hamidreza Babakhani, MSc³; Akbar Shafiee, MD, MSc⁴; Mohammad Sadeghian, MD⁵

¹Department of Cardiology, Imam Khomeini Hospital, Tehran University of Medical Sciences, Tehran, Iran

²Department of Internal Medicine, Faculty of Medicine, Rafsanjan University of Medical Sciences, Rafsanjan, Iran

³Department of Mechanical Engineering, Tarbiat Modares University, Tehran, Iran

⁴Department of Cardiovascular Research, Tehran Heart Center, Cardiovascular Diseases Research Institute, Tehran University of Medical Sciences, Tehran, Iran

⁵Department of Interventional Cardiology, Tehran Heart Center, Cardiovascular Diseases Research Institute, Tehran University of Medical Sciences, Tehran, Iran

Abstract

Background: Measurement of fractional flow reserve (FFR) is the gold standard for determining the physiologic significance of coronary artery stenosis, but newer software programs can calculate the FFR from 2-dimensional angiography images.

Methods: A retrospective analysis was conducted using the records of patients with intermediate coronary stenoses who had undergone adenosine FFR (aFFR). To calculate the computed FFR, a software program used simulated coronary blood flow using computational geometry constructed using at least 2 patient-specific angiographic images. Two cardiologists reviewed the angiograms and determined the computational FFR independently. Intraobserver variability was measured using κ analysis and the intraclass correlation coefficient. The correlation coefficient and Bland-Altman plots were used to assess the agreement between the calculated FFR and the aFFR.

Results: A total of 146 patients were included, with 95 men and 51 women, with a mean (SD) age of 61.1 (9.5) y. The mean (SD) aFFR was 0.847 (0.072), and 41 patients (27.0%) had an aFFR of 0.80 or less. There was a strong intraobserver correlation between the computational FFRs ($r = 0.808$; $P < .001$; $\kappa = 0.806$; $P < .001$). There was also a strong correlation between aFFR and computational FFR ($r = 0.820$; $P < .001$) and good agreement on the Bland-Altman plot. The computational FFR had a high sensitivity (95.1%) and specificity (90.1%) for detecting an aFFR of 0.80 or less.

Conclusion: A novel software program provides a feasible method of calculating FFR from coronary angiography images without resorting to pharmacologically induced hyperemia.

Keywords: Atherosclerosis; angiography, coronary; coronary artery disease; fractional flow reserve, myocardial

Introduction

Fractional flow reserve (FFR) measurement is used in interventional cardiology to determine the physiologic significance of coronary artery stenosis and to eliminate the discrepancy between anatomy and physiology.^{1,2} Patients with coronary artery disease (CAD) who have an FFR greater than 0.8 are typically considered for conservative medical treatment, and those with an FFR of 0.8 or less benefit from revascularization.³ Despite the valuable diagnostic yield of the FFR in patients with CAD, it is not widely used because of its expense and the technical difficulties and longer procedural time involved.^{4,5} Yet FFR-guided percutaneous coronary intervention (PCI)

Citation: Mohammadi V, Ghasemi M, Rahmani R, Mehrpooya M, Babakhani H, Shafiee A, Sadeghian M. Validity and diagnostic performance of computing fractional flow reserve from 2-dimensional coronary angiography images. *Tex Heart Inst J*. 2023;50(1):e207410. doi:10.14503/THIJ-20-7410

Corresponding author: Mohammad Sadeghian, MD, Tehran Heart Center, North Kargar Av, Tehran, 1411713138, Iran (msadeghian@tums.ac.ir)

© 2023 by The Texas Heart® Institute, Houston

The Texas Heart Institute Journal • 2023, Vol. 50, No. 1

<https://doi.org/10.14503/THIJ-20-7410> 1 / 8

<http://prime-pdf-watermark.prime-prod.pubfactory.com/> | 2025-02-09

yields better clinical outcomes and lowers costs for the healthcare system, a particular concern in developing countries.⁶⁻⁸

Traditionally, FFR has been measured by inducing hyperemia via coronary administration of adenosine (aFFR) and contrast media.⁹ In recent years, computed tomography (CT)-derived FFR has been introduced as a useful noninvasive method of computational FFR measurement. However, it requires patients to undergo an additional procedure when they may already have coronary angiography results available or when they may already be scheduled for percutaneous coronary intervention.¹⁰⁻¹² Therefore, interpretation of coronary angiography images for FFR measurement is of great value. The feasibility of using nonhyperemic images for frame counting and computing FFR has been demonstrated before.¹³ However, some data show that computing FFR using noninvasive 2-dimensional (2D) quantitative coronary angiography is feasible¹⁴ because of advances in digital programming and processing of angiography images. A previous article described testing of a computational model for measuring FFR noninvasively using angiographic images.¹⁵ This study aimed to retrospectively validate the FFR values derived from software that used 2D coronary artery angiography images in patients with CAD against aFFR measurements obtained during coronary angiography, and to assess the diagnostic performance of this modality.

Patients and Methods

Study Population

Patients who underwent coronary angiography at Imam Khomeini Hospital or Bahman Hospital in Tehran between March 2017 and March 2019 were eligible for study inclusion. The sample size was calculated based on the results of a previous study with an estimated sensitivity of 74%, specificity of 99%, and prevalence of 33% for an FFR of 0.80 or lower.¹⁵ All patients were candidates for FFR measurement, according to the judgment of their interventional cardiologist, because of borderline angiographic lesions in the coronary arteries. All patients were age 19 years or older and underwent elective coronary angiography with aFFR measurement. The exclusion criteria were a history of revascularization (by either percutaneous coronary angiography or coronary artery bypass graft surgery), a history of valvular disease or valvular surgery, and low-quality angiographic images. The institutional research board and the medical ethics committee of Imam Khomeini Hospital Complex and the board of directors at Bahman Hospital approved the study's protocol (IR.TUMS.IKHC.

Abbreviations and Acronyms

2D	2-dimensional
3D	3-dimensional
aFFR	adenosine fractional flow reserve
CAD	coronary artery disease
cFFR	computational fractional flow reserve
CT	computed tomography
dia	diameter
FAST	fractional flow reserve angiographic scoring tool
FFR	fractional flow reserve
hype	hyperemia
Pa	pressure of the aortic root
Pd	arterial pressure distal to the area of stenosis
TFC	Thrombolysis in Myocardial Infarction frame count
TIMI	Thrombolysis in Myocardial Infarction

REC.1397.005). Based on institutional routine, all participants signed written informed consent at the time of hospital admission that permitted the anonymous use of their clinical data for research purposes.

Measurements

A detailed history and physical examination were obtained after admission. Each patient's medical history, medications, comorbidities, and presence of cardiovascular risk factors—including hypertension, diabetes mellitus, hyperlipidemia, and smoking—were recorded.

Angiography

Angiography was performed in the catheterization laboratory at both centers by the same cardiologist, using similar standard protocols. All angiographic procedures were performed via femoral access by an expert interventionist. Patients were assessed physiologically before intervention, and then intracoronary nitroglycerin (25-200 µg) and intravenous unfractionated heparin (100 IU/kg) were injected. The guiding catheter was placed in the relevant coronary artery, and a 0.014 pressure wire was advanced distal to the area of stenosis; the arterial pressure distal to the coronary stenosis and the aortic root pressure were measured to calculate their ratio. Intravenous adenosine was injected to induce hyperemia, and aFFR was measured. A default FFR value of less than 0.8 was used to select stenoses for intervention.

Calculation of Noninvasive FFR

A single x-ray angiography image was selected for each patient to determine the size of the coronary stenosis. The external diameter of the contrast-filled catheter (5F or 6F) was used as the calibration standard for the right and left coronary arteries. The projection demonstrating the stenosis with the least foreshortening was used, and the stenosis diameter, lesion length, distal diameter, and proximal diameter in the end-diastolic frame were manually selected using DICOM viewer software (MicroDicom Ltd). To convert pixel size to mm, a scaling factor was determined. Angiography was performed using manual injection of contrast dye, and images were acquired digitally at the speed of 15 frames/s.

The Thrombolysis in Myocardial Infarction (TIMI) frame count (TFC) was used to assess flow across the stenotic region in the angiographic images. Using the TFC method, the number of frames required for the dye to reach a distal landmark was counted. The contrast transport time in the target branch of the coronary artery was calculated using rest projections based on the TFC. The mean flow rate at rest was derived using the mean length of the coronary artery divided by the contrast transport time, multiplied by the reference cross-sectional area.

Maximum hyperemia was simulated by modeling the resistance-reducing effect of adenosine on the downstream coronary arteries. Wilson et al showed that, for arteries in which the resistance would be expected to be minor (both at rest and during hyperemia), total coronary resistance at maximum hyperemia falls to 0.21 times the resting value with intravenous administration of 140 mg/kg/min of adenosine.¹⁶

The force driving blood flow is the pressure gradient in the coronary artery. Mean arterial pressure, which

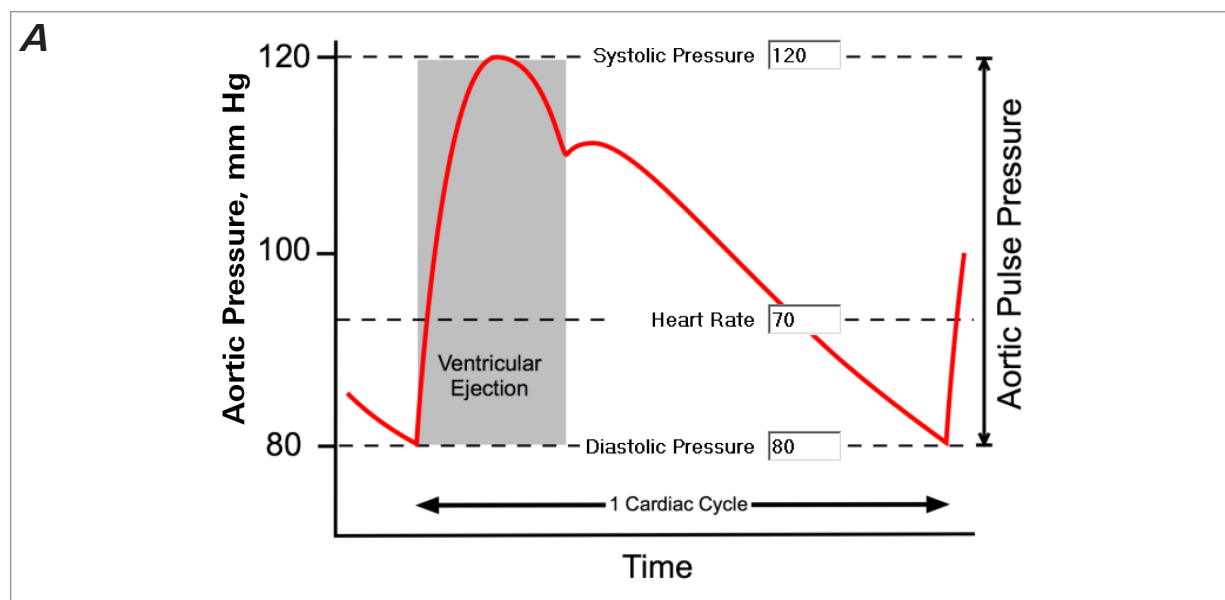
represents the average pressure over the cardiac cycle, is responsible for driving blood into the distal vessels and ultimately into the tissues. The model selected a diastolic pressure of 80 mm Hg, a systolic pressure of 120 mm Hg, and a heart rate of 70/min for all patients.

The analytical model used to calculate FFR was derived from energy conservation and considered the convection and diffusive energy losses as well as the energy loss caused by sudden constriction and expansion in the lumen area. The model captured the relation between pressure drop across a vessel and blood flow through it. Under the assumptions that the flow is steady (laminar flow) and the vessel is rigid and uniform, resistance can be quantified using steady law, which relates resistance to the geometry (length and radius) of the vessel and the blood viscosity. A detailed description of the mathematical model and computational method of the software used in this study has been published elsewhere.¹⁵ An example of computational FFR measurement using the study software is depicted in Figure 1.

Two cardiologist researchers reviewed the angiograms and independently measured computational FFR values. They were unaware of each other's findings. The computational FFRs were compared to measure the intraobserver variability, and the mean computational FFR was used for validation. The computational FFR values were compared with the measured aFFR values.

Statistical Analysis

Continuous variables were described as the mean (SD). The Kolmogorov-Smirnov test was used to test the normality of continuous data. Categorical variables were described as frequency (percentage). The intraobserver correlation of the computational FFR measurements and the correlation between the mean computational



B

Frame -3 Frame -2 Frame -1
 Frame 0 Frame 1 Frame 2 Short Conventional

Angiography Device Frame Number

15 frame / s 25 frame / s 30 frame / s

Coronary Arteries

Left Anterior Descending (LAD)
 Left Circumflex Artery (LCX)
 Right Coronary Artery (RCA)

Timi Frame Count (Rest) Timi Frame Count (Hype)

C

Catheter Diameter

French Catheter Scale

5 French 6 French 7 French

Proximal Diameter Distal Diameter
 Stenosis Dia (SD1) Lesion Length
 Stenosis Dia (SD2)

Result

Area Stenosis (%)
 Significant

Diameter Stenosis (%)
 Borderline

Assessment

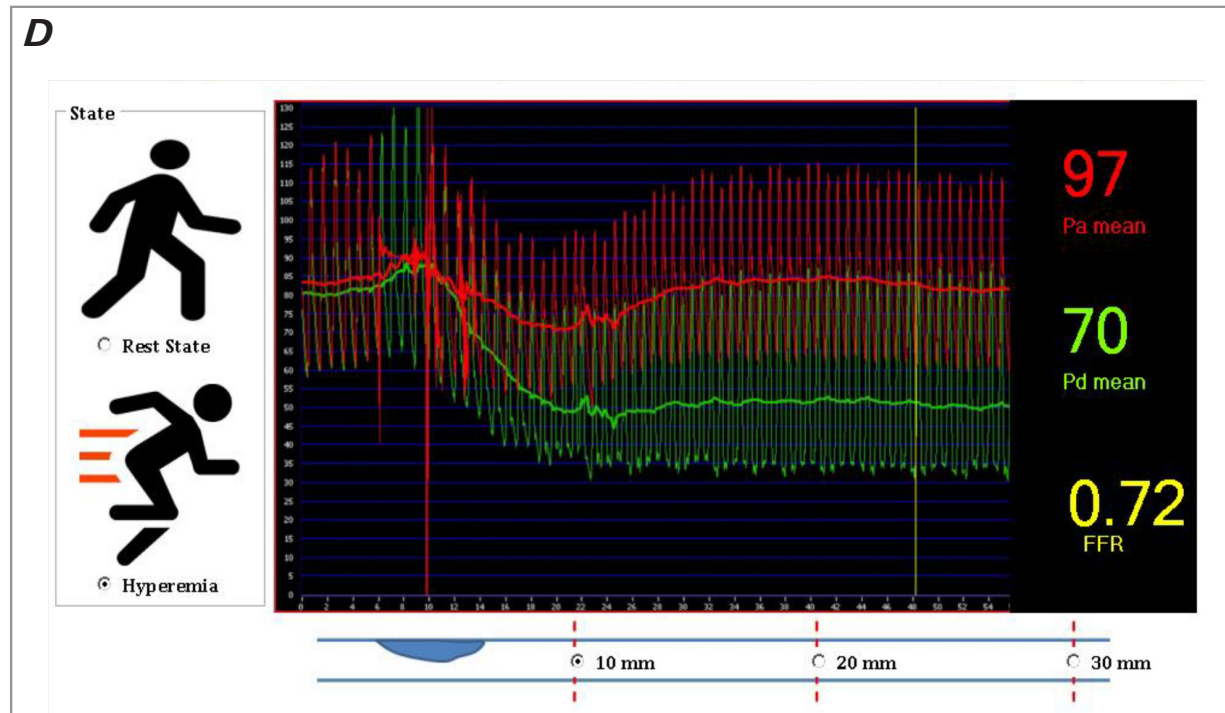


Fig. 1 A sample computation of FFR using the study software; **A)** mean arterial pressure is calculated for all patients using a diastolic pressure of 80 mm Hg, systolic pressure of 120 mm Hg, and a heart rate of 70; **B)** The number of frames required for the dye to reach a distal landmark is counted, and the contrast transport time in the target coronary artery branch during hyperemia is calculated based on the rest projections using the TFC method; **C)** An angiographic image from each patient is selected for calculating coronary stenosis; the external diameter of the contrast-filled catheter (eg, 5F, 6F) is used as the calibration standard for the right and left coronary arteries, and a scaling indicator is used to convert pixels to mm; **D)** FFR is calculated using the study software.

Dia, diameter; FFR, fractional flow reserve; hype, hyperemia; Pa, pressure of the aortic root; Pd, arterial pressure distal to the area of stenosis; TFC, Thrombolysis in Myocardial Infarction frame count; TIMI, Thrombolysis in Myocardial Infarction.

FFR and the aFFR were calculated using Spearman's correlation analysis. A κ analysis and the intraclass correlation coefficient were used to test agreement between the 2 observers. Bland-Altman plots were used to assess the agreement between the computational FFR and aFFR. Sensitivity, specificity, positive predictive value, and negative predictive value for computational FFR were calculated. Statistical analyses were performed using SPSS software, version 21.0 (IBM) and MedCalc software, version 13.3.3.3 (MedCalc Software). A P value of less than .05 was considered statistically significant.

Results

A total of 621 patients underwent FFR measurement at the study centers during the relevant time frame; 528 patients met study criteria, and 146 were selected at random for study inclusion. The mean (SD) patient age was 61.1 (9.5) years; 95 patients (65.1%) were men and 51 patients (34.9%) were women. Patients' general

characteristics and frequency of classic cardiovascular risk factors are described in Table I.

The most common culprit vessel was the left anterior descending artery (79.6%), followed by the right coronary, circumflex, and left main coronary arteries. The mean (SD) aFFR was 0.847 (0.072), and 41 patients (27.0%) had an FFR of 0.80 or less (Table II). There was a strong correlation between the independently measured computational FFRs ($r = 0.808$; $P < .001$). The κ statistic for the operators was 0.806 ($P < .001$), demonstrating excellent agreement. The intraclass correlation coefficient for the operators was 0.912 (95% CI, 0.879-0.936). There was a strong correlation between the aFFR and the computational FFR ($r = 0.820$; $P < .001$). The Bland-Altman plot also showed good agreement between the 2 methods (Fig. 2). The software-derived computational FFR based on coronary angiography images had a high sensitivity (95.1%) and specificity (90.1%) for detecting an aFFR of 0.80 or less (Table III).

TABLE I. General Characteristics of the Study Population

Characteristic	Value (N = 146)
Age, mean (SD), y	61.1 (9.5)
Male / female sex, No. (%)	95 (65.1) / 51 (34.9)
Diabetes mellitus, No. (%)	30 (20.5)
Dyslipidemia, No. (%)	16 (10.9)
Hypertension, No. (%)	31 (21.2)
Smoking, No. (%)	22 (15.0)

TABLE II. Angiographic Characteristics and Values of Conventional and Software-Derived Fractional Flow Reserve

Characteristic	Value (N = 146)
Culprit vessel, No. (%)	
LAD	121 (79.6)
RCA	21 (13.8)
LCX	7 (4.6)
LM	3 (2.0)
FFR, mean (SD), %	0.847 (0.072)
FFR \leq 0.8, %	41 (27.0)
Noninvasive FFR, operator 1, mean (SD), %	0.826 (0.080)
Noninvasive FFR $<$ 0.80, operator 1	47 (30.9)
Noninvasive FFR, operator 2, mean (SD), %	0.827 (0.087)
Noninvasive FFR $<$ 0.80, operator 2	52 (34.2)
Noninvasive FFR, mean (SD), %	0.827 (0.081)
Noninvasive FFR $<$ 0.80, mean (SD)	50 (32.9)

FFR, fractional flow reserve; LAD, left anterior descending artery; LCX, left circumflex artery; LM, left main coronary artery; RCA, right coronary artery.

Discussion

Angiographic measurement of FFR is invasive and poses technical and clinical difficulties.^{17,18} Noninvasive FFR calculation needs to implement various sophisticated computational and mathematical methods; several methods have been proposed to date. The obvious advantage of all these methods is their feasibility in all settings, their elimination of the need to use pressure guide wires, and the reproducibility of their results. In a previous simulation study, the computational model used in the present study was tested in 85 patients with stable CAD. The current study demonstrates the feasibility and diagnostic performance of this software for

TABLE III. Diagnostic Performance of Software-Derived Noninvasive Flow Ratio Using Coronary Angiography for Predicting Fractional Flow Reserve \leq 0.8

Characteristic	Value, % (95% CI)
Sensitivity	95.1 (82.1-99.1)
Specificity	90.1 (82.5-94.7)
Positive predictive value	78.0 (63.6-88.0)
Negative predictive value	98.0 (92.4-99.6)
Diagnostic accuracy	91.4 (85.8-95.3)

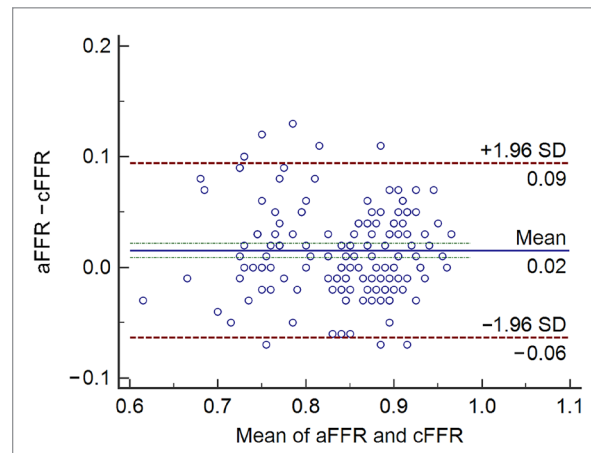


Fig. 2 The Bland-Altman graph uses the mean values for adenosine fractional flow reserve and noninvasive (computational) fractional flow reserve; there is good correlation and agreement between the measurements.

aFFR, adenosine fractional flow reserve; cFFR, computational fractional flow reserve.

measuring FFR noninvasively using coronary angiographic images; this method is able to detect FFR with high sensitivity and specificity.

Earlier studies in this field tried to use predictive tools to improve both diagnostic power and selection of intermediate lesions that require FFR measurement. The FFR Angiographic Scoring Tool (FAST) uses 4 independent angiographic variables: quantitative coronary angiography percentage-diameter stenosis, length greater than 20 mm, stenosis haziness, and multivessel disease.¹⁹ A score of 2 or lower indicates FFR of 0.80 or less with a negative predictive value of 96.5% and a sensitivity of 93.8%. Despite the validation of the FAST score, its use requires extra effort and time from an expert to reach a definite diagnostic value. In 2014, Tu et al¹³ designed a model to calculate quantitative FFR from 3-dimensional (3D) coronary angiography and TFCs. This noninvasive method is able to diagnose an

FFR of 0.80 or less with a diagnostic accuracy of 88%, and there is a strong correlation between the quantitative FFR and wired aFFR values ($r = 0.81$). However, the relatively small number of participants in this study limits conclusions about the sensitivity and specificity of this method. Also, the method requires considerable time for computing the FFR and should be performed only by an expert cardiologist.

The same authors published a prospective multicenter pilot study (FAVOR) comparing 3 different flow models for measuring quantitative FFR.²⁰ They found that a contrast-flow quantitative flow ratio that does not require pharmacologically induced hyperemia yields results similar to those of aFFR and can potentially be used to assess coronary lesions. Another study developed and validated a virtual method for FFR measurement using geometric vessel data from rotational coronary angiography images.²¹ The results indicate that FFR can quickly be measured virtually on a personal computer with high accuracy. Nevertheless, this method requires complex measurements that are not available at every facility and that are not cost-effective, including rotational coronary angiography and measurement of coronary microvascular resistance using an invasive pressure wire.²² In one study, quantitative FFR was successfully measured in 306 intermediate coronary lesions using Suite XA/QAngio XA 3D/quantitative flow ratio software (Medis Medical Imaging).²³ In this method, a 3D model of the target vessel was reconstructed from 2 angiographic projections to compute the quantitative flow ratio. An FFR of 0.80 or less was detected with a sensitivity of 0.74 and specificity of 0.83.

A multicenter study of 301 patients (319 vessels) used a methodology similar to that of the present study and showed very high sensitivity and specificity for angiographic FFR, with a diagnostic accuracy of greater than 90% for predicting the reference standard, aFFR.¹⁴ Moreover, a recent quantitative meta-analysis showed that quantitative FFR is a simple, useful, and noninvasive modality that can diagnose functionally important intermediate coronary artery stenoses with a sensitivity of 0.89 and specificity of 0.88.²⁴ The results of the present study are in line with all the above studies and show that noninvasive FFR measurement in patients with stable CAD is feasible and reliable.

Another noninvasive modality that can assess FFR based on computational fluid dynamics and image-based modeling is CT angiography.^{2,24,25} However, CT-FFR does not perform well with advanced and calcific coronary lesions, previously implanted stents, arrhythmias, inadequate image quality, or motion artifacts.^{12,26} Moreover, it is not available everywhere, and the interpretation and use of CT images requires considerable expertise. Therefore,

precise image processing, elimination of artifacts, and acquisition of necessary data for computation are of great importance in computational FFR measurement from angiogram images. The method used in the present study uses computational fluid dynamics derived from 2D images of conventional coronary angiography without induction of pharmacologic hyperemia. Data regarding the superiority of angiographic images for FFR computation are still limited; only 1 prior study has shown that 1-dimensional blood flow models derived from intravascular ultrasonography can provide an accurate and quick prediction of FFR compared with the 3D simulations provided by CT images.²⁷ More studies are required to compare noninvasive FFR measurements derived from angiography images and CT images.

Study Limitations

This was a retrospective study, and the angiograms were acquired for clinical diagnostic purposes, not research purposes. The quality of the angiograms was not satisfactory in a few instances, as they were not recorded according to noninvasive FFR image acquisition guidelines. Therefore, a prospective study with professional standards for obtaining high-quality angiographic images is needed before this technology is ready for widespread use. The validity of this study method for assessing coronary arteries with venous grafts, previously revascularized arteries, and other anatomical variances is unknown. The time required for operators to measure FFR using the study software was not recorded but was less than 10 minutes for the well-trained operators. The results of this study are preliminary and need to be validated by larger studies.

Conclusion

The software program used in this study provides a feasible and rapid method of computing FFR from coronary angiography images without pharmacologically induced hyperemia. These results build on the body of reliable evidence for the practicality of computational FFR measurement using 2D coronary angiographic images. However, more studies are required before this method can be used in routine practice. Collaboration between all scientists in this field, and pooling of available data, can lead to the development of a globally approved software program.

Published: 31 January 2023

Conflict of Interest Disclosures: None

Funding/Support: This study was supported by Imam Khomeini Hospital, Tehran University of Medical Sciences, Tehran, Iran.

References

1. Collet C, Onuma Y, Sonck J, et al. Diagnostic performance of angiography-derived fractional flow reserve: a systematic review and Bayesian meta-analysis. *Eur Heart J*. 2018;39(35):3314-3321. doi:10.1093/eurheartj/ehy445
2. Cook CM, Petraco R, Shun-Shin MJ, et al. Diagnostic accuracy of computed tomography-derived fractional flow reserve: a systematic review. *JAMA Cardiol*. 2017;2(7):803-810. doi:10.1001/jamacardio.2017.1314
3. De Bruyne B, Pijls NH, Kalesan B, et al; FAME 2 Trial Investigators. Fractional flow reserve-guided PCI versus medical therapy in stable coronary disease. *N Engl J Med*. 2012;367(11):991-1001. doi:10.1056/NEJMoa1205361
4. Toth GG, Toth B, Johnson NP, et al. Revascularization decisions in patients with stable angina and intermediate lesions: results of the international survey on interventional strategy. *Circ Cardiovasc Interv*. 2014;7(6):751-759. doi:10.1161/CIRCINTERVENTIONS.114.001608
5. van Rosendaal AR, Koning G, Dimitriu-Leen AC, et al. Accuracy and reproducibility of fast fractional flow reserve computation from invasive coronary angiography. *Int J Cardiovasc Imaging*. 2017;33(9):1305-1312. doi:10.1007/s10554-017-1190-3
6. Quintella EF, Ferreira E, Azevedo VMP, et al. Clinical outcomes and cost-effectiveness analysis of FFR compared with angiography in multivessel disease patient. *Arq Bras Cardiol*. 2019;112(1):40-47. doi:10.5935/abc.20180262
7. Sengottuvelu G, Chakravarthy B, Rajendran R, Ravi S. Clinical usefulness and cost effectiveness of fractional flow reserve among Indian patients (FIND study). *Catheter Cardiovasc Interv*. 2016;88(5):E139-E144. doi:10.1002/ccd.25517
8. Stella SF, Polanczyk CA, Arvandi M, Siebert U. Cost utility of fractional flow reserve-guided percutaneous coronary intervention in multivessel coronary artery disease in Brazil. *Int J Qual Health Care*. 2019;31(9):676-681. doi:10.1093/intqhc/mzy240
9. Rahmani R, Ramezani M, Shafiee A. The influence of low and iso-osmolar contrast media on diagnostic performance of contrast fractional flow reserve measurement. *Turk Kardiyol Dern Ars*. 2022;50(4):264-269. doi:10.5543/tkda.2022.21273
10. Collet C, Miyazaki Y, Ryan N, et al. Fractional flow reserve derived from computed tomographic angiography in patients with multivessel CAD. *J Am Coll Cardiol*. 2018;71(24):2756-2769. doi:10.1016/j.jacc.2018.02.053
11. Hu X, Yang M, Han L, Du Y. Diagnostic performance of machine-learning-based computed fractional flow reserve (FFR) derived from coronary computed tomography angiography for the assessment of myocardial ischemia verified by invasive FFR. *Int J Cardiovasc Imaging*. 2018;34(12):1987-1996. doi:10.1007/s10554-018-1419-9
12. Mathew RC, Gottbrecht M, Salerno M. Computed tomography fractional flow reserve to guide coronary angiography and intervention. *Interv Cardiol Clin*. 2018;7(3):345-354. doi:10.1016/j.iccl.2018.03.008
13. Tu S, Barbato E, Köszegi Z, et al. Fractional flow reserve calculation from 3-dimensional quantitative coronary angiography and TIMI frame count: a fast computer model to quantify the functional significance of moderately obstructed coronary arteries. *JACC Cardiovasc Interv*. 2014;7(7):768-777. doi:10.1016/j.jcin.2014.03.004
14. Fearon WF, Achenbach S, Engstrom T, et al; FAST-FFR Study Investigators. Accuracy of fractional flow reserve derived from coronary angiography. *Circulation*. 2019;139(4):477-484. doi:10.1161/CIRCULATIONAHA.118.037350
15. Sadeghian M, Mohammadi V, Shafiee A, Babakhani H. Non-invasive flow ratio (NiFR) measurement based on angiography images. *J Biomed Phys Eng*. 2021;11(6):685-692. doi:10.31661/jbpe.v0i0.1160
16. Wilson RF, Wyche K, Christensen BV, Zimmer S, Laxson DD. Effects of adenosine on human coronary arterial circulation. *Circulation*. 1990;82(5):1595-1606. doi:10.1161/01.cir.82.5.1595
17. Christou MA, Siontis GCM, Katritsis DG, Ioannidis JPA. Meta-analysis of fractional flow reserve versus quantitative coronary angiography and noninvasive imaging for evaluation of myocardial ischemia. *Am J Cardiol*. 2007;99(4):450-456. doi:10.1016/j.amjcard.2006.09.092
18. Lotfi A, Jeremias A, Fearon WF, et al; Society of Cardiovascular Angiography and Interventions. Expert consensus statement on the use of fractional flow reserve, intravascular ultrasound, and optical coherence tomography: a consensus statement of the Society of Cardiovascular Angiography and Interventions. *Catheter Cardiovasc Interv*. 2014;83(4):509-518. doi:10.1002/ccd.25222
19. Hoole SP, Seddon MD, Poulter RS, Starovoytov A, Wood DA, Saw J. Development and validation of the fractional flow reserve (FFR) angiographic scoring tool (FAST) to improve the angiographic grading and selection of intermediate lesions that require FFR assessment. *Coron Artery Dis*. 2012;23(1):45-50. doi:10.1097/MCA.0b013e32834e4f71
20. Tu S, Westra J, Yang J, et al; FAVOR Pilot Trial Study Group. Diagnostic accuracy of fast computational approaches to derive fractional flow reserve from diagnostic coronary angiography: the international multicenter FAVOR pilot study. *JACC Cardiovasc Interv*. 2016;9(19):2024-2035. doi:10.1016/j.jcin.2016.07.013
21. Morris PD, Silva Soto DA, Feher JFA, et al. Fast virtual fractional flow reserve based upon steady-state computational fluid dynamics analysis: results from the VIRTU-Fast study. *JACC Basic Transl Sci*. 2017;2(4):434-446. doi:10.1016/j.jacbs.2017.04.003
22. Kern MJ, Yu JH, Seto AH. Building a fast virtual fractional flow reserve: reductionists or dreamers? *JACC Basic Transl Sci*. 2017;2(4):447-449. doi:10.1016/j.jacbs.2017.07.005
23. Kołtowski Ł, Zaleska M, Maksym J, et al. Quantitative flow ratio derived from diagnostic coronary angiography in assessment of patients with intermediate coronary stenosis: a wire-free fractional flow reserve study. *Clin Res Cardiol*. 2018;107(9):858-867. doi:10.1007/s00392-018-1258-7
24. Xing Z, Pei J, Huang J, Hu X, Gao S. Diagnostic performance of QFR for the evaluation of intermediate coronary artery stenosis confirmed by fractional flow reserve. *Braz J Cardiovasc Surg*. 2019;34(2):165-172. doi:10.21470/1678-9741-2018-0234
25. Taylor CA, Fonte TA, Min JK. Computational fluid dynamics applied to cardiac computed tomography for noninvasive quantification of fractional flow reserve: scientific basis. *J Am Coll Cardiol*. 2013;61(22):2233-2241. doi:10.1016/j.jacc.2012.11.083
26. Fan GX, Han RS, Luo JC, Huang BS, Jiang T, Wang JK. Noninvasive measurement of coronary fractional flow reserve: an under-exploiting newland. *Chin Med J (Engl)*. 2015;128(12):1695-1699. doi:10.4103/0366-6999.158383
27. Blanco PJ, Bulant CA, Müller LO, et al. Comparison of 1D and 3D models for the estimation of fractional flow reserve. *Sci Rep*. 2018;8(1):17275. doi:10.1038/s41598-018-35344-0